

## ORIGINAL ARTICLE

## Early-life lead exposure recapitulates the selective loss of parvalbumin-positive GABAergic interneurons and subcortical dopamine system hyperactivity present in schizophrenia

KH Stansfield<sup>1</sup>, KN Ruby<sup>1</sup>, BD Soares<sup>1</sup>, JL McGlothan<sup>1</sup>, X Liu<sup>2</sup> and TR Guilarte<sup>1</sup>

Environmental factors have been associated with psychiatric disorders and recent epidemiological studies suggest an association between prenatal lead (Pb<sup>2+</sup>) exposure and schizophrenia (SZ). Pb<sup>2+</sup> is a potent antagonist of the *N*-methyl-D-aspartate receptor (NMDAR) and converging evidence indicates that NMDAR hypofunction has a key role in the pathophysiology of SZ. The glutamatergic hypothesis of SZ posits that NMDAR hypofunction results in the loss of parvalbumin (PV)-positive GABAergic interneurons (PVGI) in the brain. Loss of PVGI inhibitory control to pyramidal cells alters the excitatory drive to midbrain dopamine neurons increasing subcortical dopaminergic activity. We hypothesized that if Pb<sup>2+</sup> exposure in early life is an environmental risk factor for SZ, it should recapitulate the loss of PVGI and reproduce subcortical dopaminergic hyperactivity. We report that on postnatal day 50 (PN50), adolescence rats chronically exposed to Pb<sup>2+</sup> from gestation through adolescence exhibit loss of PVGI in SZ-relevant brain regions. PV and glutamic acid decarboxylase 67 kDa (GAD67) protein were significantly decreased in Pb<sup>2+</sup> exposed rats with no apparent change in calretinin or calbindin protein levels suggesting a selective effect on the PV phenotype of GABAergic interneurons. We also show that Pb<sup>2+</sup> animals exhibit a heightened locomotor response to cocaine and express significantly higher levels of dopamine metabolites and D2-dopamine receptors relative to controls indicative of subcortical dopaminergic hyperactivity. Our results show that developmental Pb<sup>2+</sup> exposure reproduces specific neuropathology and functional dopamine system changes present in SZ. We propose that exposure to environmental toxins that produce NMDAR hypofunction during critical periods of brain development may contribute significantly to the etiology of mental disorders.

*Translational Psychiatry* (2015) 5, e522; doi:10.1038/tp.2014.147; published online 10 March 2015

## INTRODUCTION

Schizophrenia (SZ) is a devastating mental disorder believed to be the result of an adverse neurodevelopmental event with the clinical expression of the disease in adolescent and young adults.<sup>1,2</sup> Estimates of concordance in monozygotic twins are ~50%, indicating that both genetic and environmental factors are important in the etiology of SZ.<sup>3–5</sup> From an environmental perspective, various aspects of the broad environment, such as nutritional deficiency, obstetric complications and influenza outbreaks, have been implicated in the etiology of SZ.<sup>3,6,7</sup> However, the possibility that human exposures to environmental toxins during critical periods of brain development may have a role in the etiology of SZ and related mental disorders has not been studied to a significant degree.

Since the early 1970s, epidemiological studies originating from different parts of the world have consistently demonstrated detrimental associations of childhood lead (Pb<sup>2+</sup>) exposure on children's intelligence, learning ability and neuropsychological development.<sup>8–25</sup> During the last decade, studies have provided evidence that childhood Pb<sup>2+</sup> intoxication is also associated with psychiatric disorders including major depression, anxiety, delinquency or conduct disorder, and SZ in adolescent and young adults who were exposed to Pb<sup>2+</sup> as children.<sup>19–25</sup> Human neuroimaging studies in Pb<sup>2+</sup> exposed adolescent/young adults

that have been followed since infancy support the epidemiological findings with evidence of gray matter and myelin changes in brain regions affected in mental disorders.<sup>26–31</sup> In particular, the medial prefrontal cortex (mPFC) and hippocampus (HIP) appear to be the two brain regions that are consistently affected in both Pb<sup>2+</sup> exposed children and in SZ.<sup>26–29</sup> Therefore, there is substantial evidence to suggest that developmental Pb<sup>2+</sup> exposure produces detrimental effects on brain structures and neuronal systems in children and adolescents that may influence the expression of mental disorders across the lifespan.

The recent association between prenatal Pb<sup>2+</sup> exposure and an increased risk of SZ later in life<sup>24,25</sup> prompted us to propose that this association has a neurobiological underpinning, hypoactivity of the NMDA receptor (NMDAR) complex.<sup>32</sup> Further, our recent study using transgenic mice expressing the human mutant form of the SZ risk gene disrupted-in-schizophrenia 1 (DISC1), that were chronically exposed to Pb<sup>2+</sup> during development, revealed behavioral abnormalities and brain structural changes as a result of the gene–environment interaction that were consistent with a SZ phenotype.<sup>33</sup> Combined, these human and animal studies provide important evidence that environmental toxins like Pb<sup>2+</sup> that are NMDAR antagonists and have been historically present in the global environment may interact with SZ risk genes and may be involved in the etiology of mental disorders or alter the temporal expression and/or severity of the disease.

<sup>1</sup>Department of Environmental Health Sciences, Mailman School of Public Health, Columbia University, New York, NY, USA and <sup>2</sup>Department of Biostatistics, Mailman School of Public Health, Columbia University, New York, NY, USA. Correspondence: Dr TR Guilarte, Department of Environmental Health Sciences, Mailman School of Public Health, Columbia University, 722 West 168th Street, Room 1105-E, New York, NY 10032, USA. E-mail: trguilarte@columbia.edu

Received 17 September 2014; revised 25 November 2014; accepted 19 December 2014

The glutamatergic hypothesis of SZ posits that hypoactivity of the glutamatergic system, and specifically of the NMDAR has an important role in the pathophysiology of SZ.<sup>34–36</sup> There is extensive evidence that  $Pb^{2+}$  is a potent and selective antagonist of the NMDAR<sup>37–41</sup> and chronic exposure to  $Pb^{2+}$  in early life arrests the developmental NR2B-to-NR2A NMDAR subunit switch in the rat brain.<sup>40,41</sup> This is important because maturation and refinement of many brain circuits is coincident with the NMDAR subunit switch.<sup>42–45</sup> One example relevant to the present study is that of medial ganglionic eminence-derived parvalbumin (PV)-positive GABAergic interneurons (PVGI) that undergo NR2B-to-NR2A subunit switch with a functional change in their firing rate from slow to fast signaling properties.<sup>45</sup> In general, dysregulation of this important developmental NMDAR subunit switch is associated with neurological and mental disorders. Consistent with this notion, the  $Pb^{2+}$  induced arrest of the NMDAR subunit switch during brain development is associated with impaired synaptic plasticity in the form of long-term potentiation in the HIPP and deficits in cognitive function in the adolescent rat brain.<sup>46,47</sup>

One of the most robust and consistent findings documented in postmortem brain tissue from SZ subjects and in NMDAR antagonist animal models of SZ is the loss of PVGI in the mPFC and HIPP.<sup>48–53</sup> PVGI are fast-spiking GABAergic inhibitory neurons that synchronize pyramidal cell firing in the mPFC and HIPP, giving rise to gamma oscillations that are critical for cognitive function.<sup>54,55</sup> Alterations in the gamma oscillations in SZ contribute significantly to the cognitive impairments characteristic of the disease.<sup>56,57</sup> Consistent with this notion, genetic and pharmacological studies in experimental animals support an important role of the NMDAR in PVGI function. For example, genetic ablation of the NR1 subunit of the NMDAR in forebrain PVGI<sup>58</sup> or the administration of NMDAR antagonists<sup>59–63</sup> results in the loss of PV and glutamic acid decarboxylase (GAD67), markers for GABAergic interneurons in the rodent brain.

One functional consequence of the loss or dysfunction of PVGI in the mPFC and HIPP is the emergence of a behavioral phenotype consistent with diverse symptoms in SZ.<sup>34,50</sup> Psychosis, the most characteristic positive symptom in SZ has been linked to subcortical dopaminergic (DAergic) hyperactivity<sup>64</sup> and hyperactivity of subcortical DAergic neurons is a consistent finding in drug-naïve SZ patients measured by PET imaging.<sup>65–68</sup> Animal studies have shown that excess dopamine (DA) in the striatum can be induced by abnormal activity of pyramidal cells in the mPFC and HIPP by reducing their GABAergic inhibitory control.<sup>69,70</sup> Therefore, the loss or dysfunction of inhibitory PVGI control to principal neurons in the mPFC and HIPP would be expected to result in disinhibition of pyramidal cells, the loss of their synchronized firing, altering the excitatory drive to midbrain dopamine neurons increasing subcortical DAergic activity.<sup>34</sup> On the basis of this knowledge, we sought to determine whether chronic developmental  $Pb^{2+}$  exposure (1) alters the density of PVGI in SZ-relevant regions of the adolescent rat brain and (2) affects subcortical dopaminergic activity.

## MATERIALS AND METHODS

### Animal care and animal husbandry

All animal studies were approved by the Columbia University Medical Center Animal Care and Use Committee and have been carried out in accordance with the Guide for Care and Use of Laboratory Animals as stated by the U.S. National Institutes of Health. The adult female Long-Evans rats (Charles River, Bar Harbor, ME, USA; 250 g) were fed 0 p.p.m. (control) or 1500 p.p.m. lead acetate in the diet (RMH 1000; Dyets, Bethlehem, PA, USA). The female rats were bred to normal Long-Evans males and litters were culled to 10 on postnatal day 1 (PN1). Pups were weaned on PN21 and fed the same diet as their respective dams. At postnatal day 50 (PN50), one male rat from each control or  $Pb^{2+}$  exposed

litter was killed and the brain harvested for analysis. Blood  $Pb^{2+}$  concentrations at PN50 were measured using the LeadCare system (ESA Laboratories, Chelmsford, MA, USA).

### Antibodies

Primary antibodies against PV (1:1000; Rabbit Polyclonal, ab11427, Abcam, Cambridge, MA, USA), Actin (1:1000; Goat Polyclonal, sc-1616, Santa Cruz Biotechnology, Santa Cruz, CA, USA), GAD67 (1:1000; Mouse Monoclonal, ab26116, Abcam), calretinin (1:1000 Abcam; ab702, Abcam) and 1:1000 calbindin (1:1000; Abcam, ab11426, Abcam) were used. Goat anti-rabbit biotinylated secondary antibody (1:200) and avidin–biotin–peroxidase complex (1:50) solution were purchased from Vector Laboratories (Burlingame, CA, USA). Corresponding fluorophore conjugated  $10 \mu\text{g ml}^{-1}$  Alexa Fluor 488 and Alexa Fluor 594 was purchased from Molecular Probes (Eugene, OR, USA). Appropriate fluorescent secondary antibodies were purchased for western blotting (IRDye800 and IRDye 680, LI-COR Biosciences, Lincoln, NE, USA).

### Brain tissue preparation

For immunostaining, rats were transcardially perfused with 200 ml phosphate buffer followed by 500 ml of 4% paraformaldehyde in 0.1 M phosphate buffer. Brains were removed and post-fixed for 24 h in 4% paraformaldehyde before being cryoprotected with 30% sucrose and flash frozen with 2-methylbutane. Brains were cut into 40- $\mu\text{m}$  thick sections in the coronal plane through the frontal cortex, striatum and HIPP using a freezing microtome (Leica SM2000R; Leica Microsystems, Wetzlar, Germany). For fresh frozen tissue, brains were harvested, rinsed in saline and frontal cortex, HIPP and striatum dissected for western blot or the whole brain was kept intact for quantitative receptor autoradiography studies.

### Immunohistochemistry and immunofluorescence

Free-floating tissue sections were rinsed with Tris-buffered saline (TBS) followed by pre-treatment with 0.6%  $\text{H}_2\text{O}_2$  for 20 min, rinsed with TBS, pre-treated with 0.4% Triton X-100 for 45 min, blocked with 5% normal goat serum for 1 h before being incubated with PV (1:1000) for 24 h at 4 °C. After rinsing with TBS, sections were incubated with goat anti-rabbit biotinylated secondary IgG for 1 h at room temperature followed by incubation with the avidin–biotin–peroxidase complex (1:50) for 30 min. The reaction product was visualized using 3,3'-diaminobenzidine (DAB), 0.03%  $\text{H}_2\text{O}_2$  with or without 0.04%  $\text{NiCl}_2$ . Sections were mounted and dehydrated before being coverslipped using Permount media. For immunofluorescence, sections were incubated with the primary antibodies: PV and GAD67 followed by incubation in corresponding fluorophore-conjugated secondary antibodies overnight at 4 °C. Sections were mounted and coverslipped using pro-long antifade serum (Molecular Probes).

### Protein harvesting and western blot

For PV, GAD67, calretinin and calbindin western blots; frontal cortex, striatal and HIPP tissue from control and  $Pb^{2+}$  exposed PN50 rats were lysed in radioimmunoprecipitation assay buffer containing 150 mM NaCl, 50 mM Tris, 5 mM EGTA, 1% Triton, 5% deoxycholate and 20% SDS. Western blot membranes were incubated in the appropriate primary antibodies: 1:1000 PV (Abcam, ab11427), 1:500 GAD67 (Abcam, ab97739), 1:1000 calretinin (Abcam, ab702), 1:1000 calbindin (Abcam, ab11426) and 1:1000 Actin (Santa Cruz Biotechnology, sc-1616) diluted in blocking solution overnight at 4 °C. The membranes were visualized using the Odyssey imaging system (LI-COR). Integrated intensity of the protein of interest was normalized to  $\beta$ -actin levels from the same blot.

### Stereological cell counting of parvalbumin-positive cells

All slides were coded and the experimenter was masked for cell counting. Boundaries for primary motor cortex (M1), mPFC (including the infralimbic, prelimbic and cingulate regions), caudal, middle and rostral areas of the striatum and the dentate gyrus, CA1, CA2, CA3 and CA4 regions of the pyramidal cell layer of the HIPP were defined using a  $\times 4$  objective lens. All PVGI within the outlined areas were counted using a  $\times 40$  oil immersion lens on an Olympus BX51 Microscope using Visiopharm software (Hoersholm, Denmark). Cell density (Nv) was calculated using the equations published in Dorph-Petersen *et al.*<sup>71</sup>

### Locomotor activity measurement and drug-dosing paradigm

At PN50, control or Pb<sup>2+</sup> exposed rats were placed into one of three experimental groups for the administration of saline, 5 mg kg<sup>-1</sup> or 15 mg kg<sup>-1</sup> cocaine-HCL. Before injection, all the rats were placed in an automated activity chamber (Digiscan Animal Activity Monitor, Omnitech Electronics) and locomotor activity was recorded for 60 min to allow for behavioral habituation. After 60 min had elapsed, the rats were administered a single intraperitoneal injection of saline, 5 mg kg<sup>-1</sup> cocaine-HCL or 15 mg kg<sup>-1</sup> cocaine-HCL before being placed back in the activity chamber for an additional 60 min to monitor locomotor activity. Total distance traveled was measured.

### High-performance liquid chromatography analysis of dopamine and metabolites

Rat striatum was sonicated in 500 µl of 0.1 N perchloric acid before being centrifuged at 14 000 r.p.m. for 20 min at 4 °C according to the method of Sheleg *et al.*<sup>72</sup> The pellets were dried overnight at 30 °C and the supernatants were filtered through 0.22-µm filters before being injected onto a high-performance liquid chromatography with electrochemical detection (Waters, Milford, MA, USA) for neurochemical analysis of DA and its metabolites, 3,4-dihydroxyphenylacetic acid (DOPAC) and homovanillic acid (HVA). The components were separated on a cation exchange column CMD-150 X 3.2 column; ESA Biosciences, Chelmsford, MA, USA) using an isocratic mobile phase (CMD-TM mobile phase; ESA Biosciences) including 2.2 mM NaCl pumped at a constant flow rate of 0.5 ml min<sup>-1</sup>. DA, DOPAC and HVA were quantified by electrochemical detection using a glossy carbon-working electrode with a 2.0-mm diameter *in situ* silver reference electrode (flow cell, 2 mm GC WE, ISAC, Waters). Dried pellets were sonicated and dissolved in a final concentration of 0.1 N NaOH and the protein concentration for each sample was determined using a bicinchoninic acid assay reagent kit (Pierce, Rockford, IL, USA) and measured on a Spectramax microplate reader (Molecular Devices, Sunnyvale, CA, USA). Data are expressed in ng per mg of protein.

### D2-dopamine receptor (D2R), dopamine transporter (DAT) and vesicular monoamine transporter-type 2 (VMAT-2) quantitative autoradiography

Fresh-frozen brains were sliced at 20-micron thickness on a cryostat (Leica Biosystems) and mounted on poly-L-lysine-coated slides, and stored at -20 °C until used for quantitative receptor autoradiography.

#### D2R autoradiography

Tissue slides were incubated in 3 nM [<sup>3</sup>H]-Raclopride in Tris-HCl buffer (pH 7.4) for 30 min at room temperature for total binding. Nonspecific binding was determined in the presence of 10 µM haloperidol (D2R antagonist). The slides were then washed three times in buffer at 4 °C for 1 min, and then quickly dipped in dH<sub>2</sub>O at 4 °C and left to dry overnight.

#### VMAT-2 autoradiography

Tissue slides were pre-washed in 20 mM HEPES-sucrose buffer for 15 min at room temperature. For total binding, slides were incubated in HEPES-sucrose buffer containing 7.5 nM [<sup>3</sup>H]-dihydrotetrabenazine (DTBZ) for 1 h. Nonspecific binding was determined by adding 2 µM unlabeled DTBZ. The slides were then washed three times in Tris-HCl-sucrose buffer for 5 min at room temperature, and quickly dipped in dH<sub>2</sub>O at 4 °C and left to dry overnight.

#### DAT autoradiography

Tissue slides were pre-washed in 50 mM Tris-HCl buffer for 20 min at room temperature. For total binding, slides were incubated in Tris-HCl buffer containing 5 nM [<sup>3</sup>H]-Win 35 428 for 90 min at room temperature. Nonspecific binding was determined by adding 2 µM GBR-12909 (DAT antagonist). The slides were then washed three times in buffer at 4 °C for 5 s, and quickly dipped in dH<sub>2</sub>O at 4 °C and left to dry overnight.

After drying, D2R, VMAT-2 and DAT slides were apposed to KODAK BioMax MR film, MR-1, along with [<sup>3</sup>H]-Microscales (Amersham, Arlington Heights, IL, USA), for 6–7 weeks. Reference standards were included with each film to ensure linearity of optical density and to allow quantitative analysis of the images. Images were captured, digitized and optical density was quantified (MCID, InterFocus Imaging, Cambridgeshire, UK). All autoradiography for D2R, VMAT-2 and DAT was conducted using slides of coronal brain sections that represented the following areas: rostral

striatum (Bregma 1.60 mm), middle striatum (Bregma -0.26 mm), caudal striatum (Bregma -0.92 mm), nucleus accumbens core and nucleus accumbens shell (Bregma 1.60 mm). A rat brain atlas was used to define distinct striatal regions (The Rat Brain in Stereotaxic Coordinates, 4th edition). Imaging software in MCID was used to delineate and measure binding intensity in the different regions of the striatum.

### Statistical analysis

To examine treatment effect defined as mean difference between specific treatment groups, we calculated mean and s.e.m. for region-specific PVGI by treatment group, and used two-sample *t*-test to detect treatment group difference in PVGI density in specific brain regions. Brain dopamine and metabolite concentrations were analyzed using a two-sample *t*-test to detect treatment group differences between control and Pb<sup>2+</sup> exposed samples. Size of treatment effect was documented by Cohen's *d*. To adjust *P*-values for multiple tests, Holm's Bonferroni step-down method was used. The same statistical analysis was performed with SAS software 9.3 for the treatment effect in the quantitative receptor autoradiography results. Locomotor data were analyzed using a two-way analysis of variance.

## RESULTS

### Blood lead levels and body weight of rats

As previously described by us, this Pb<sup>2+</sup> exposure paradigm does not produce an overt toxic effect on the body weight as we did not find a significant effect of the chronic Pb<sup>2+</sup> exposure of the body weight of rats at PN50. That is, the body weight of control rats was 336 ± 13 g (mean ± s.e.m.; *n* = 30) and Pb<sup>2+</sup> exposed rats body weight was 313 ± 11 g (mean ± s.e.m.; *n* = 30; *P* = 0.2). At PN50, the resulting blood Pb<sup>2+</sup> levels in these animals was 22.2 ± 0.9 µg dl<sup>-1</sup> (*n* = 47) for Pb<sup>2+</sup> exposed rats and 0.6 ± 0.1 µg dl<sup>-1</sup> (*n* = 64) for control rats, a difference that was highly significant (*P* < 0.0001).

### Identification and stereological cell counting of parvalbumin-positive GABAergic interneurons in the rat brain

Immunofluorescent double-label confocal imaging of PV and GAD67 showed that PV co-labeled with GAD67, but not all GAD67-labeled neurons co-labeled with PV, consistent with the fact that only a fraction of the total pool of GABAergic interneurons has a PV phenotype (Figure 1b). Stereological cell counting of PVGI was performed in the mPFC and in the primary motor cortex (M1; Figures 1a, c and d). In the M1, stereological cell counting indicates a significant treatment effect (*P* = 0.014) with the density of PVGI in M1 being significantly lower in Pb<sup>2+</sup> treated rats relative to controls. The mean ± s.e.m. density of PVGI in control animals was 5342 ± 401 cells mm<sup>-3</sup> (*n* = 6) and 3442 ± 502 cells mm<sup>-3</sup> (*n* = 6) in Pb<sup>2+</sup> treated animals (35.6% reduction; Figure 1d). We also observed a significant (*P* = 0.005) decrease in the density of PVGI in the mPFC of Pb<sup>2+</sup> animals relative to controls (Figures 1c and d). The mean ± s.e.m. density of PVGI in the mPFC of control animals was 9938 ± 584 cells mm<sup>-3</sup> (*n* = 6); and 6432 ± 636 cells mm<sup>-3</sup> (*n* = 6) in Pb<sup>2+</sup> exposed animals (35.3% reduction). Western blots of frontal cortex tissue confirmed the cell counting results as we observed a significant decrease (20.6%) in PV (control: *n* = 4; Pb<sup>2+</sup>: *n* = 5; *P* = 0.035) and GAD67 protein PV (25.8% decrease; control: *n* = 4; Pb<sup>2+</sup>: *n* = 5; *P* = 0.035) in Pb<sup>2+</sup> treated animals relative to controls (Figure 2).

To determine whether Pb<sup>2+</sup> exposure affected PVGI density in other brain regions relevant to SZ, we performed stereological cell counting in the striatum and in the pyramidal and granule cell layers of the HIPP. In the HIPP, when pyramidal and granule cell layer cell counts were combined, there was an overall (total) Pb<sup>2+</sup> treatment effect on mean PVGI density that was statistically significantly different relative to controls (*P* = 0.0004). The mean ± s.e.m. density of PVGI in the HIPP of control animals was 3072 ± 101 cells mm<sup>-3</sup> (*n* = 7) and 2064 ± 181 cells mm<sup>-3</sup> (*n* = 7) in Pb<sup>2+</sup> animals (32.8% reduction; Figures 3b and c). The

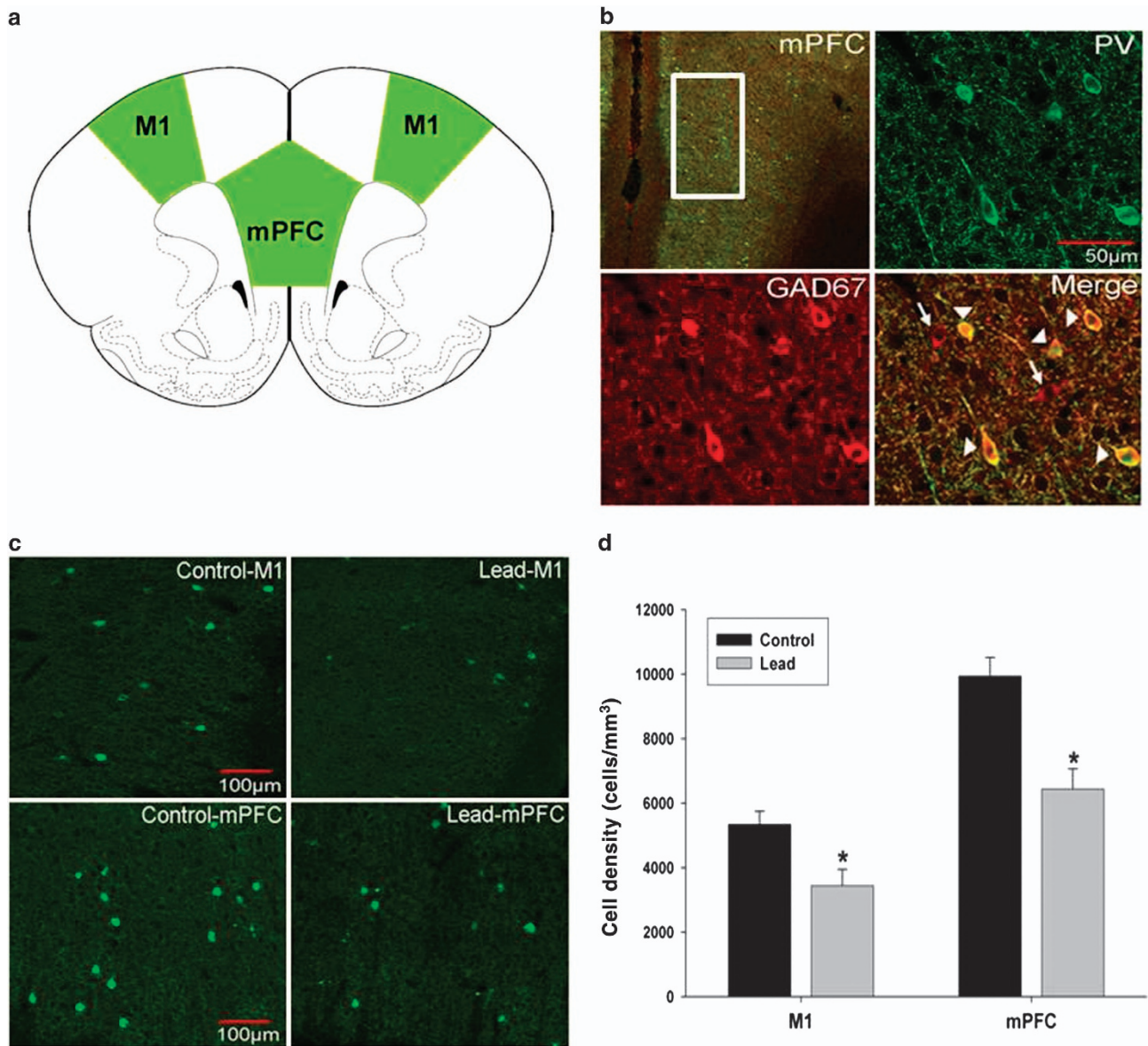


**Figure 1.** Parvalbumin-positive cell density in the primary motor cortex (M1) and medial prefrontal cortex (mPFC) of control and  $Pb^{2+}$  treated rats. (a) Rat atlas depictions of frontal cortex regions traced in green and used for PVGI cell counting. (b) Parvalbumin-positive interneurons (PV, green) in the mPFC co-labeled with GAD67 (red). However, not all GAD67-labeled cells co-labeled with PV consistent with the fact that only a portion of GABAergic interneurons are PV positive. Arrowheads point to PV and GAD67 co-labeled cells. Arrows point to GAD67-positive cells that do not co-label with PV. (c) Representative fluorescence confocal images of PVGI from control and  $Pb^{2+}$  treated animals. (d) PVGI cell density was significantly lower in M1 and mPFC of  $Pb^{2+}$  animals compared with controls. Data are represented as the mean  $\pm$  s.e.m. \*, significantly different from control. PVGI, parvalbumin-positive GABAergic interneurons.

examination of different HIPP subregions showed that the overall  $Pb^{2+}$  treatment effect on PVGI density was driven by a highly significant change in the CA3 region ( $P=0.0032$ ), with marginal changes in the CA2 region ( $P=0.085$ ; Figure 3c). In addition, the levels of PV ( $P=0.041$ , 11% reduction) and GAD67 ( $P=0.004$ , 31% reduction) protein measured by western blot were significantly reduced in the HIPP from  $Pb^{2+}$  treated rats relative to controls, confirming the cell counting results (Figure 2).

In the striatum, PVGI density count was performed in the rostral, middle and caudal aspects of the striatum and these regions were averaged as the whole striatum (Figure 4c). The mean  $\pm$  s.e.m. density of PVGI in the whole striatum from control animals was  $716 \pm 43$  cells  $mm^{-3}$  ( $n=9$ ) and  $612 \pm 26$  cells  $mm^{-3}$  ( $n=7$ ) in  $Pb^{2+}$

animals (Figure 4c). The differences in the striatum as a whole were not significantly different ( $P=0.057$ ). However, analysis of the rostral, middle and caudal aspects of the striatum individually revealed that the greatest effect of  $Pb^{2+}$  was in the caudal aspects of the striatum where a highly significant decrease in PVI density was observed ( $P=0.014$ ; Figure 4c). The mean  $\pm$  s.e.m. density of PVGI in the caudal striatum of control animals was  $676 \pm 56$  cells  $mm^{-3}$  ( $n=9$ ) and  $460 \pm 24$  cells  $mm^{-3}$  ( $n=7$ ) in  $Pb^{2+}$  treated animals representing a 32% reduction in PVGI density (Figure 4c). Similar to the frontal cortex and HIPP, we found significantly lower levels of PV ( $P=0.0039$ , ~27% reduction) and GAD67 ( $P=0.0033$ , ~22% reduction) protein in the striatum of  $Pb^{2+}$  animals compared with controls by western blot (Figure 2).

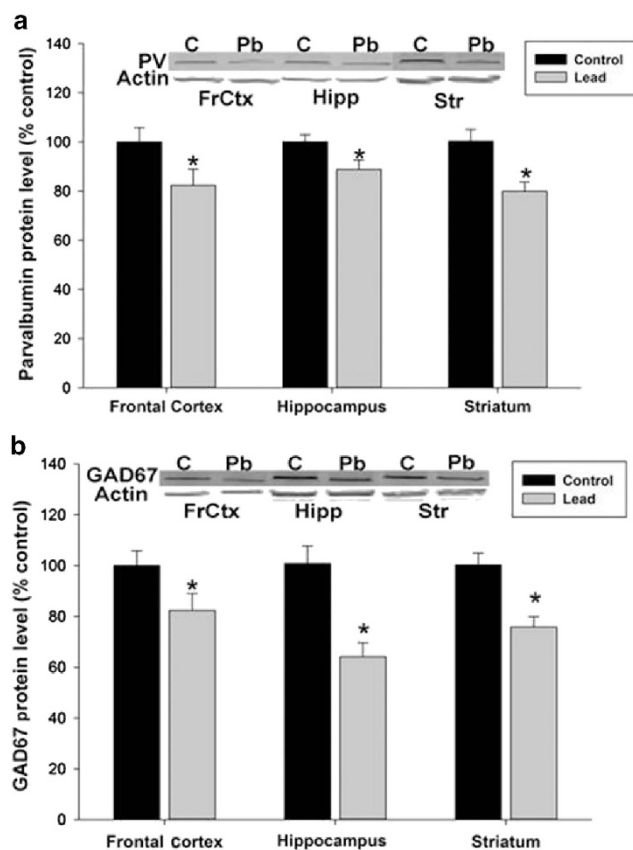


**Figure 2.** Parvalbumin (PV) and GAD67 protein expression in the frontal cortex (FrCtx), hippocampus (Hipp) and striatum (Str). Western blot revealed a significant reduction in PV (a) and GAD67 (b) protein expression in the frontal cortex (PV: 20% reduction,  $P=0.04$ , GAD67: 20% reduction,  $P=0.04$ ), hippocampus (PV: 15% reduction,  $P=0.04$ , GAD67: 35% reduction,  $P=0.003$ ) and striatum (PV: 20% reduction,  $P=0.003$ ; GAD67: 25% reduction,  $P=0.003$ ) of Pb<sup>2+</sup> treated rats ( $n=5$ ) relative to controls ( $n=4$ ). Integrated intensity of the protein of interest was normalized to  $\beta$ -actin levels from the same blot and compared with controls and represented as a percentage. Data are presented as the mean  $\pm$  s.e.m. \*, significantly different from control.

#### Subcortical dopaminergic activity and D2-dopamine receptor levels in the striatum

The loss or dysfunction of PVGI in the mPFC and HIPP has been shown to affect subcortical DA system activity.<sup>34,50,69,73</sup> Therefore, to determine whether Pb<sup>2+</sup> exposed animals expressed functional subcortical DAergic system changes, we administered cocaine to control and Pb<sup>2+</sup> exposed animals and measured their locomotor response. Cocaine is a psychostimulant that enhances synaptic DA levels by blocking DAT in the striatum.<sup>74</sup> Locomotor activity (total distance traveled) was measured for 60 min in control and Pb<sup>2+</sup> exposed rats before and after saline or a low (5 mg kg<sup>-1</sup>) or high (15 mg kg<sup>-1</sup>) intraperitoneal cocaine dose.

Figure 5a shows that Pb<sup>2+</sup> exposed animals had an increased locomotor response to cocaine (saline: 731  $\pm$  82 cm,  $n=14$ ; 5 mg kg<sup>-1</sup>: 1750  $\pm$  366 cm,  $n=11$ ; 15 mg kg<sup>-1</sup>: 5786  $\pm$  531 cm,  $n=23$ ) compared with control animals (saline: 655  $\pm$  116 cm,  $n=11$ ; 5 mg kg<sup>-1</sup>: 802  $\pm$  144 cm,  $n=10$ ; 15 mg kg<sup>-1</sup>: 3192  $\pm$  529 cm,  $n=18$ ) (drug dose main effect:  $F(2,81)=36.25$ ,  $P<0.001$ ; Pb<sup>2+</sup> dose main effect:  $F(2,81)=9.470$ ,  $P=0.002$ ; interaction:  $F(2,81)=3.54$ ,  $P=0.03$ ). It should be noted that at all doses of cocaine, the locomotor response of Pb<sup>2+</sup> exposed animals was significantly

higher than controls. Further, the 5 mg kg<sup>-1</sup> dose of cocaine did not elicit a locomotor response in control animals, whereas it had a robust locomotor response in Pb<sup>2+</sup> exposed animals (Figure 5a). The data indicate that Pb<sup>2+</sup> exposed rats express a functionally hyperactive subcortical DAergic system.

A hallmark feature of SZ is increased levels of D2R and increased DA release in the striatum. To assess the effect of Pb<sup>2+</sup> exposure on these DAergic markers, we performed quantitative receptor autoradiography using the D2R ligand [<sup>3</sup>H]-raclopride and high-performance liquid chromatography with electrochemical detection of DA and metabolites in the striatum. We found significantly higher concentrations of the DA metabolites DOPAC (208% increase;  $P=0.0009$ ) and HVA (146% increase;  $P=0.016$ ) in the striatum of Pb<sup>2+</sup> exposed rats relative to controls (Figure 5b), whereas DA ( $P=0.089$ ), DOPAC/DA ( $P=0.099$ ) and HVA/DA ( $P=0.099$ ) ratio did not reach statistical significance after adjusting for multiple comparisons (Figure 5b). Our results also revealed that Pb<sup>2+</sup> animals had an overall higher level of [<sup>3</sup>H]-raclopride-specific binding in the striatum (averaged dorsal and ventral striatum) than control rats ( $P=0.0242$ ; Figure 5d). The mean  $\pm$  s.e.m. of [<sup>3</sup>H]-raclopride-specific binding in the striatum of control animals was 53.1  $\pm$  1.9 fmol mg<sup>-1</sup> tissue ( $n=7$ ) and 58.7  $\pm$  0.4 fmol mg<sup>-1</sup> tissue ( $n=6$ ) for Pb<sup>2+</sup> exposed animals. This change represents a 10.5% increase in the level of total striatal D2R (Figure 5d). A regional assessment of [<sup>3</sup>H]-raclopride binding to D2R between control and Pb<sup>2+</sup> exposed animals showed that the largest effect of Pb<sup>2+</sup> exposure on D2R levels occurred in the rostral aspects of the dorsal striatum (control: 55.0  $\pm$  2.0 fmol mg<sup>-1</sup> tissue ( $n=7$ ), Pb<sup>2+</sup> exposed: 63.3  $\pm$  1.8 fmol mg<sup>-1</sup> tissue ( $n=7$ );  $P=0.0494$ ) representing a 15% increase. Together, these findings indicate that chronic developmental Pb<sup>2+</sup> exposure results in a hyperactive DAergic system. We should also note that these effects of Pb<sup>2+</sup> on the cocaine-induced locomotor response and dopamine markers occurred in the absence of a change in DAT and VMAT-2 levels as measured by quantitative receptor autoradiography (Supplementary Figure 1).

#### DISCUSSION

In the present study, we show for the first time that chronic developmental exposure to Pb<sup>2+</sup> results in the loss of PVGI cell density in the mPFC, HIPP and striatum, brain regions that have been implicated in SZ. Further, the loss of PVGI is associated with hyperactivity of the subcortical DAergic system, features that are a hallmark of SZ. The effect of Pb<sup>2+</sup> exposure on PVGI cell density loss appears to be selective to the PV phenotype as the regional expression of calretinin or calbindin protein, markers for other GABAergic interneuron types, were not affected in the same animals (Supplementary Figure 2). Together, our findings suggest that the Pb<sup>2+</sup> induced decrease in GAD67 protein that we have documented in the rat brain is the result of a specific insult on PVGI.

The decrease of PVGI cell density in the frontal cortex, HIPP and striatum of Pb<sup>2+</sup> exposed animals ranges from ~32.0 to 35.6% relative to controls and is consistent with what has been observed in postmortem brain tissue from SZ subjects and in NMDAR antagonist animal models of SZ. That is, in postmortem frontal cortex and HIPP tissue from SZ subjects, reductions in PV and GAD67 gene and protein expression range in the order of 31–60% decrease,<sup>48,49,75–79</sup> with no significant effect on calretinin interneurons.<sup>48,77,80</sup> Similarly, studies using NMDAR antagonist drugs in rodents have duplicated the PV/GAD67 deficits observed in the SZ brain. For example, repeated subanesthetic doses of ketamine decreases the number of PVGI in the CA1–CA3 regions of the pyramidal cell layer by 34% and in the dentate gyrus of the HIPP by 44%.<sup>60</sup> Prenatal<sup>61</sup> and postnatal exposure<sup>81</sup> to another NMDAR antagonist, (5S,10R)-(+)-5-methyl-10,11-dihydro-5H-dibenzo[*a,d*]cyclohepten-5,10-imine maleate (MK-801), decreases

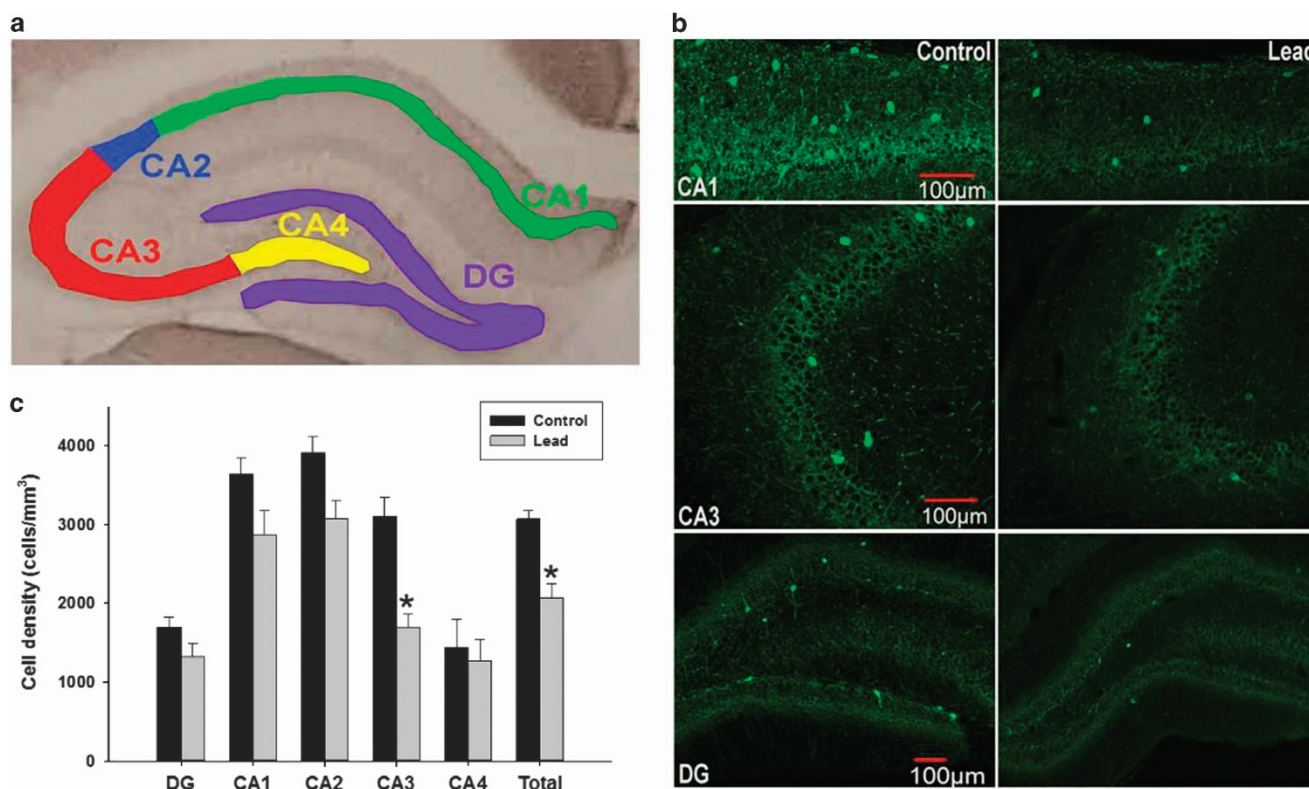


**Figure 3.** Parvalbumin-positive cell density in control and Pb<sup>2+</sup>-treated rats in the hippocampus. (a) Representative areas used for PVGI cell counting in the pyramidal CA1 (green), CA2 (blue), CA3 (red), CA4 (yellow) subregions and granule cell layer of the dentate gyrus (DG; purple). (b) Confocal imaging of immunofluorescence labeled PVGI in the CA1, CA3 and dentate gyrus. (c) PVGI cell density in the pyramidal and granule cell layers of the dorsal hippocampus. Bar designated total was the average of all hippocampal subregions. Data are represented as the mean  $\pm$  s.e.m. \*, significantly different from control.

the density of PVGI in the prefrontal cortex and HIPP of young adult rats by  $\sim$ 32%<sup>61</sup> and 31–38%,<sup>81</sup> respectively. Another study using phencyclidine-treated neonatal rats also found a 20% loss of PVGI in the mPFC.<sup>63</sup> The percent change in PVGI cell loss in these NMDAR antagonist animal models of SZ are consistent with the percent loss in the present study. Finally, Sadikot *et al.*<sup>82</sup> reported that the density of PVGI is decreased in the mature striatum when the NMDAR antagonist MK-801 is administered during the proliferation period (embryonic days 15–18) of PVGI, but observed no effect on striatal PVGI cell number if the MK-801 was administered immediately after their proliferation period (embryonic days 18–21). These findings suggest that NMDAR-mediated glutamatergic transmission has a key role in the development of PVGI. Together, they indicate that NMDAR antagonists administered at different periods of brain development result in the loss of PVGI markers in the mPFC, HIPP and striatum, consistent with SZ being a disease of neurodevelopment. It is striking that the brain regional change and magnitude of the PVGI loss in Pb<sup>2+</sup> exposed animals in the present study is similar to those described in postmortem brain samples from SZ subjects and in NMDAR antagonist animal models of SZ.

What are putative mechanism(s) by which early-life Pb<sup>2+</sup> exposure results in the loss of PVGI?

Previous work has shown that Pb<sup>2+</sup> is a potent antagonist of the NMDAR and that chronic exposure to Pb<sup>2+</sup> in early life alters the ontogeny of NMDAR subunits, with selective reductions in NR1 and NR2A subunit gene and protein expression in the adolescent rat brain.<sup>46,83</sup> These findings are relevant because genetic deletion of the NR1 subunit from forebrain PVGI shortly after birth results in the loss of PV and GAD67 in the same PVGI in which the NR1

subunit was deleted, and these animals express a behavioral phenotype consistent with SZ.<sup>58</sup> The same study also showed that the deletion of the NR1 subunit in forebrain PVGI after adolescence did not produce the same abnormalities, indicating the importance of the insult occurring in early life. Notably, in early development, PVGI exhibit higher level of NR2A–NMDAR complexes<sup>84,85</sup> with increased sensitivity to NMDAR antagonists than pyramidal cells<sup>86,87</sup> and NR2A-containing NMDAR are essential for the maintenance of PV and GAD67 protein in cultured PVGI.<sup>84</sup> Therefore, NMDAR complexes expressed on PVGI appear to be more vulnerable to a developmental insult than pyramidal cells. This is consistent with studies indicating that the NR2A subunit of the NMDAR is decreased in PVGI in the SZ brain<sup>76,88</sup> and in animals exposed to the NMDAR antagonist, MK-801.<sup>88</sup> Other evidence shows that chronic blockade of NR2A–NMDAR, but not NR2B–NMDAR complexes during development decreases PVGI density and selectively impairs inhibitory transmission from fast-spiking PVGI.<sup>89</sup> Thus, the most parsimonious explanation for why Pb<sup>2+</sup> exposure during brain development results in the loss of PVGI is that NMDAR hypoactivity induced by Pb<sup>2+</sup> inhibition results in a selective decrease of NR2A–NMDAR complexes on PVGI, reducing synaptic NR2A–NMDAR downstream signaling, leading to a loss of PVGI.<sup>84</sup>

Loss of corticolimbic and hippocampal parvalbumin-positive GABAergic interneurons results in a hyperactive subcortical dopaminergic system

As previously noted, the loss of PVGI in the frontal cortex and HIPP results in disinhibition of pyramidal cells and the loss of their synchronized firing, altering the activity of midbrain DAergic neurons.<sup>34</sup>

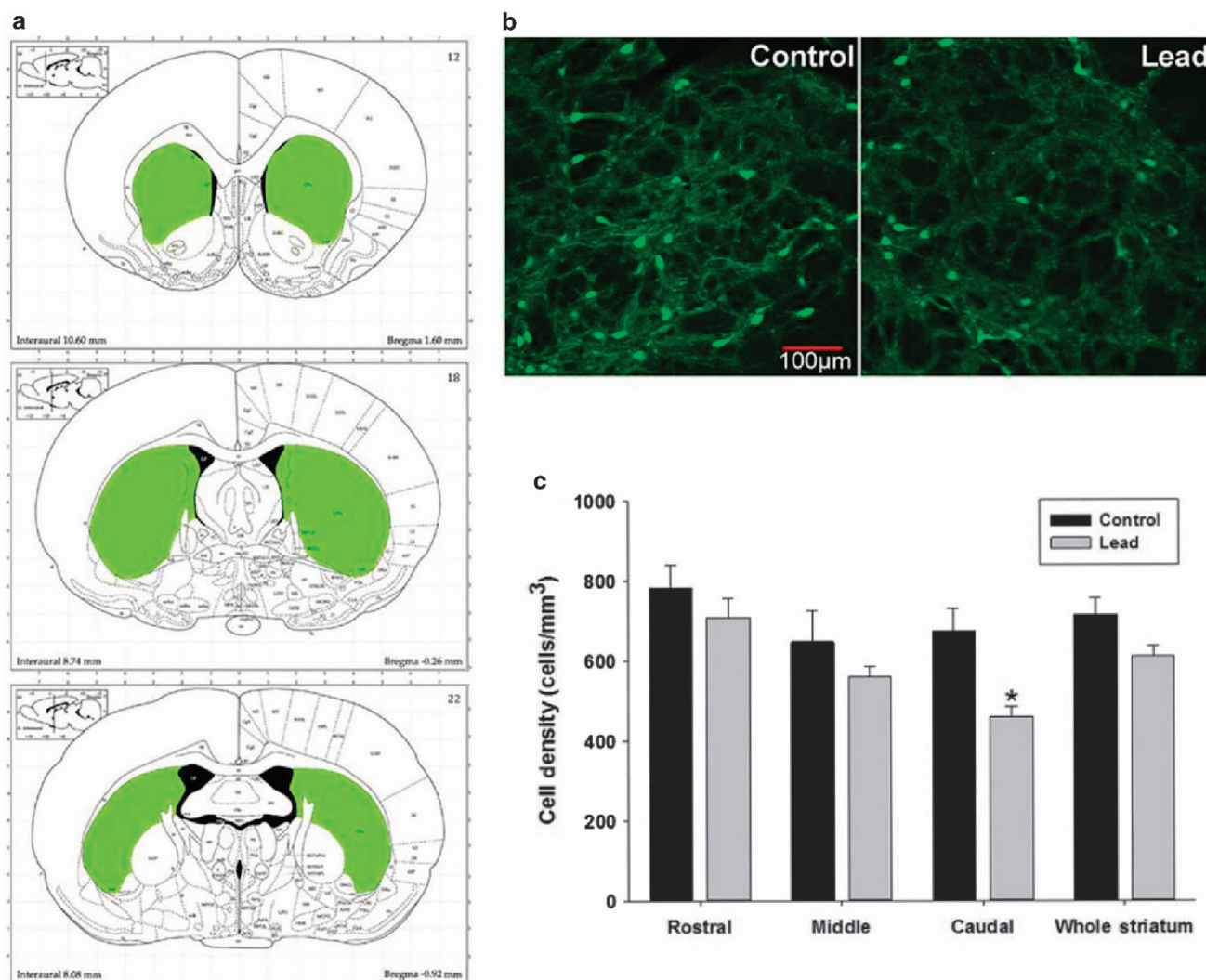


**Figure 4.** Parvalbumin-positive cell density in the striatum of control and Pb<sup>2+</sup> exposed rats. (a) Representative striatal regions used for PVGI cell counting (rostral, middle and caudal). (b) Immunofluorescence confocal imaging of PVGI in the caudal striatum from control and Pb<sup>2+</sup> exposed animals. (c) PVGI cell density results for the striatum. While there was no overall effect of Pb<sup>2+</sup> in the whole striatum when rostral, middle and caudal regions were averaged, we observed a significant decrease of PVGI in the caudal striatum of Pb<sup>2+</sup> animals relative to controls when regions were analyzed individually. Data are represented as the mean (cells) ± s.e.m. \*, significantly different from control.

To assess whether Pb<sup>2+</sup> exposed animals also expressed altered subcortical DAergic activity, we administered saline or cocaine (intraperitoneal; 5 or 15 mg kg<sup>-1</sup> body weight) to control and Pb<sup>2+</sup> exposed animals and measured their locomotor response as a functional readout of subcortical DAergic activity. Our results revealed that the locomotor response to cocaine administration was significantly higher in Pb<sup>2+</sup> exposed animals relative to controls (Figure 5a), indicative of a hyperactive DAergic system. On the basis of the locomotor response of Pb<sup>2+</sup> exposed animals to cocaine administration, we hypothesized that DA system markers were likely to be altered by Pb<sup>2+</sup> exposure and we measured striatal levels of DA, DOPAC, HVA and D2R. Quantitative receptor autoradiography using the D2R ligand [<sup>3</sup>H]-raclopride revealed that Pb<sup>2+</sup> exposed animals expressed a significant increase in D2R levels in the striatum (Figure 5d). The magnitude of the increase of D2R in the striatum of Pb<sup>2+</sup> exposed animals is similar to what has been observed in the striatum of SZ patients<sup>90</sup> and in a DISC1 rodent model of SZ.<sup>91</sup>

Analysis of DA and metabolites revealed increased levels and the DA metabolites HVA and DOPAC in the striatum (Figure 5b). This finding is consistent with an *in vivo* electrochemical study

showing dopamine overflow in the nucleus accumbens of rats exposed to similar levels of Pb<sup>2+</sup> as in the present study.<sup>92</sup> No significant changes were measured for striatal DAT and VMAT-2 in Pb<sup>2+</sup> exposed rats relative to controls indicating that the increased locomotor response to cocaine was not due to the changes in DAT or VMAT-2 (Supplementary Figure 1). Together, our results provide evidence of increased striatal metabolites indicative of increased DA turnover and increased D2R levels. These findings resemble those found in the brain of SZ subjects using PET and SPECT imaging.<sup>93</sup>

In summary, animals chronically exposed to environmentally relevant levels of Pb<sup>2+</sup> during brain development express three key features that are observed in SZ: (1) the loss of PVGI in brain regions relevant to SZ pathology, (2) subcortical DAergic hyperactivity and (3) increased levels of D2R in the striatum. The current findings combined with previous studies showing impairments of hippocampal long-term potentiation,<sup>46</sup> adult neurogenesis in the HIPP,<sup>94</sup> prepulse inhibition of the startle response<sup>95</sup> and cognitive function<sup>46,47,96</sup> in similarly Pb<sup>2+</sup> exposed and age-matched animals are consistent with what has been observed in the SZ brain and in NMDAR antagonist animal models of SZ.

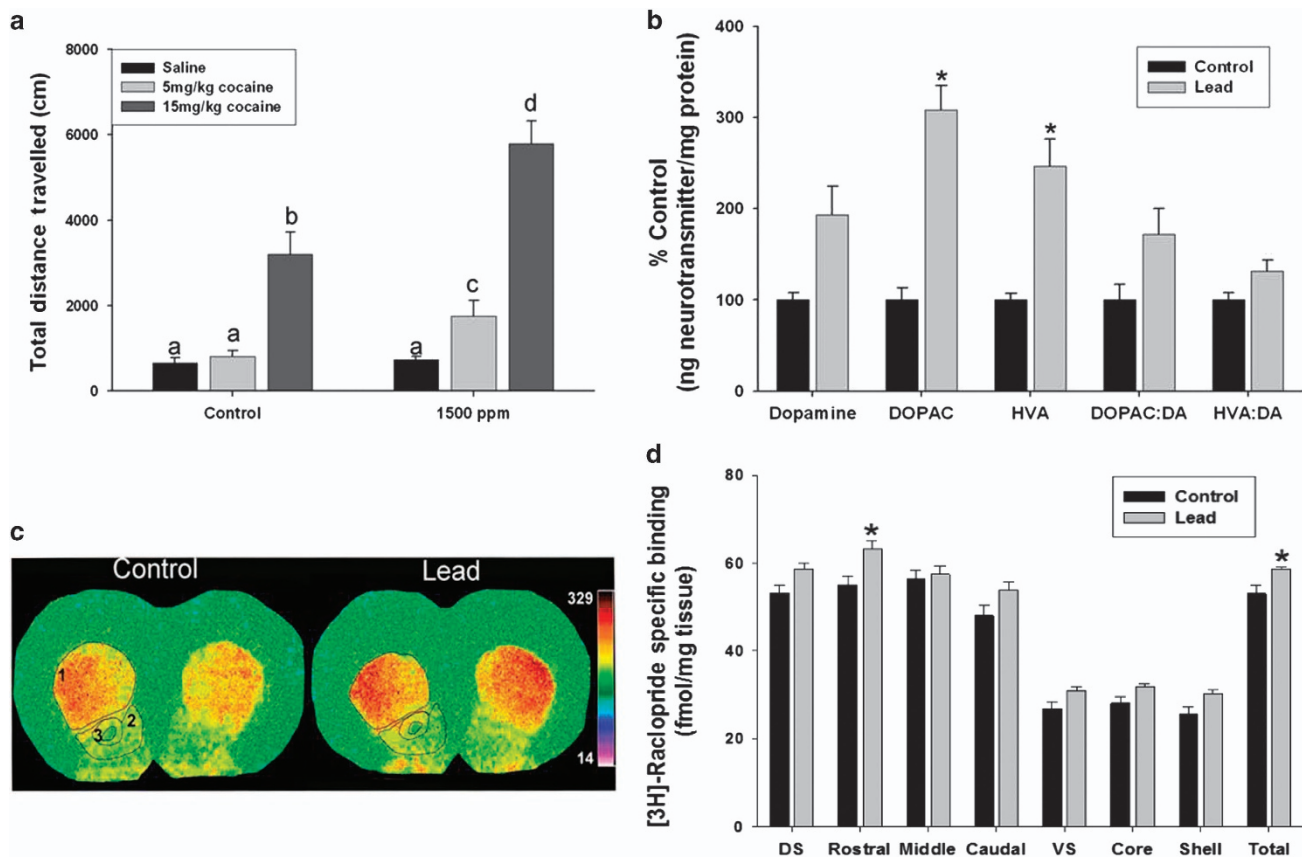


**Figure 5.** Subcortical dopamine (DA) system activity and D2R levels in the rat striatum. (a) Effect of cocaine or saline administration on the locomotor response of control and Pb<sup>2+</sup> treated animals. In a, bars with different letters are significantly different at  $P < 0.05$ . (b) High-performance liquid chromatography analysis of striatal DA and its metabolites, DOPAC and HVA were significantly increased in lead-exposed rats compared with control. In addition, the DOPAC/DA and HVA/DA ratio were significantly increased in Pb<sup>2+</sup> treated rats. Data are presented as percent control of the mean ng of neurotransmitter per mg of protein  $\pm$  s.e.m. \*, significantly different from control. (c) Representative pseudocolor autoradiographic images of [3H]-raclopride total binding to D2R in the striatum from control and Pb<sup>2+</sup> treated rats. Number labels are: 1 = dorsal striatum; 2 = nucleus accumbens shell; 3 = nucleus accumbens core. (d) [3H]-raclopride-specific binding to D2R in the dorsal and ventral striatum from control and Pb<sup>2+</sup> treated rats. Data are presented as mean (fmol mg<sup>-1</sup> tissue)  $\pm$  s.e.m. DOPAC, 3,4-dihydroxyphenylacetic acid; DS, dorsal striatum (average of rostral, middle and caudal); HVA, homovanillic acid; VS, ventral striatum (average of core and shell). \*, significantly different from control.

Last, our findings have translational implications to humans because the Pb<sup>2+</sup> exposure paradigm and the resulting levels of Pb<sup>2+</sup> in the blood of adolescent rats used in the present study are relevant to the blood Pb<sup>2+</sup> levels that have been measured for decades in a significant percentage of children not only in the United States (<http://www.cdc.gov/nceh/lead/data/StateConfirmedByYear1997-2001.htm>), but also worldwide.<sup>41,97</sup> Consistent with this notion, recent estimates by the World Health Organization indicate that Pb<sup>2+</sup> exposure accounts for 0.6% of the global burden of disease and contributes to ~600 000 new cases of children with intellectual disabilities every year ([http://www.who.int/ipcs/lead\\_campaign/en/](http://www.who.int/ipcs/lead_campaign/en/)). Further, data from the National Health and Nutrition Examination Survey (NHANES) indicate that ~1% of women of childbearing age (15–44 years) in the United States have blood Pb<sup>2+</sup> levels that are equal or greater than the current Center for Disease Control (CDC) level of concern (<http://www.cdc.gov/nceh/lead/publications/leadandpregnancy2010.pdf>). Therefore, a significant percentage of children worldwide continue to be at risk for neurodevelopmental problems resulting from Pb<sup>2+</sup> exposure during critical periods of brain development and these effects may contribute significantly to mental disorders across the lifespan.

#### CONFLICT OF INTEREST

The authors declare no conflict of interest.

#### ACKNOWLEDGMENTS

This work was supported by grants from the National Institute of Environmental Health Sciences number E5006189, ViCTER supplement to E5006189, E5020465 to TRG and a pilot project from NIEHS Center P30ES009089 to KHS. We acknowledge Dr Jason Richardson and Dr Mubarak Hossain for their assistance and allowing us to use the high-performance liquid chromatography with electrochemical detection for the analysis of dopamine and metabolites. In addition, we acknowledge Ms Michelle Obenauer for her technical assistance.

#### REFERENCES

- Weinberger DR. On the plausibility of "the neurodevelopmental hypothesis" of schizophrenia. *Neuropsychopharmacology* 1996; **14**: 15–115.
- Insel TR. Rethinking schizophrenia. *Nature* 2010; **468**: 187–193.
- Tsuang MT, Stone WS, Faraone SV. Genes, environment and schizophrenia. *Br J Psychiatry Suppl* 2001; **40**: s18–s24.
- van Os J, Kenis G, Rutten BP. The environment and schizophrenia. *Nature* 2010; **468**: 203–212.
- Brown AS. The environment and susceptibility to schizophrenia. *Prog Neurobiol* 2011; **93**: 23–58.

- 6 Brown AS, Susser ES. Prenatal nutritional deficiency and risk of adult schizophrenia. *Schizophr Bull* 2008; **34**: 1054–1063.
- 7 Munk-Jorgensen P, Ewald H. Epidemiology in neurobiological research: exemplified by the influenza-schizophrenia theory. *Br J Psychiatry Suppl* 2001; **40**: s30–s32.
- 8 Baghurst PA, McMichael AJ, Wigg NR, Vimpani GV, Robertson EF, Roberts RJ *et al*. Environmental exposure to lead and children's intelligence at the age of seven years. The Port Pirie Cohort Study. *N Engl J Med* 1992; **327**: 1279–1284.
- 9 Bellinger D, Sloman J, Leviton A, Rabinowitz M, Needleman HL, Wateraux C. Low-level lead exposure and children's cognitive function in the preschool years. *Pediatrics* 1991; **87**: 219–227.
- 10 Canfield RL, Henderson CR Jr, Cory-Slechta DA, Cox C, Jusko TA, Lanphear BP. Intellectual impairment in children with blood lead concentrations below 10 microg per deciliter. *N Engl J Med* 2003; **348**: 1517–1526.
- 11 Kordas K, Canfield RL, Lopez P, Rosado JL, Vargas GG, Cebrian ME *et al*. Deficits in cognitive function and achievement in Mexican first-graders with low blood lead concentrations. *Environ Res* 2006; **100**: 371–386.
- 12 Lanphear BP, Hornung R, Khoury J, Yolton K, Baghurst P, Bellinger DC *et al*. Low-level environmental lead exposure and children's intellectual function: an international pooled analysis. *Environ Health Perspect* 2005; **113**: 894–899.
- 13 Liu J, Li L, Wang Y, Yan C, Liu X. Impact of low blood lead concentrations on IQ and school performance in Chinese children. *PLoS One* 2013; **8**: e65230.
- 14 Needleman HL, Gunnoe C, Leviton A, Reed R, Peresie H, Maher C *et al*. Deficits in psychologic and classroom performance of children with elevated dentine lead levels. *N Engl J Med* 1979; **300**: 689–695.
- 15 Tellez-Rojo MM, Bellinger DC, Arroyo-Quiroz C, Lamadrid-Figueroa H, Mercado-Garcia A, Schnaas-Arrieta L *et al*. Longitudinal associations between blood lead concentrations lower than 10 microg/dL and neurobehavioral development in environmentally exposed children in Mexico City. *Pediatrics* 2006; **118**: e323–e330.
- 16 Tong S, Baghurst P, McMichael A, Sawyer M, Mudge J. Lifetime exposure to environmental lead and children's intelligence at 11–13 years: the Port Pirie cohort study. *BMJ* 1996; **312**: 1569–1575.
- 17 Wasserman GA, Liu X, Popovac D, Factor-Litvak P, Kline J, Wateraux C *et al*. The Yugoslavia Prospective Lead Study: contributions of prenatal and postnatal lead exposure to early intelligence. *Neurotoxicol Teratol* 2000; **22**: 811–818.
- 18 Wasserman GA, Staghezza-Jaramillo B, Shrout P, Popovac D, Graziano J. The effect of lead exposure on behavior problems in preschool children. *Am J Public Health* 1998; **88**: 481–486.
- 19 Bouchard MF, Bellinger DC, Weuve J, Matthews-Bellinger J, Gilman SE, Wright RO *et al*. Blood lead levels and major depressive disorder, panic disorder, and generalized anxiety disorder in US young adults. *Arch Gen Psychiatry* 2009; **66**: 1313–1319.
- 20 McFarlane AC, Searle AK, Van Hooff M, Baghurst PA, Sawyer MG, Galletly C *et al*. Prospective associations between childhood low-level lead exposure and adult mental health problems: the Port Pirie cohort study. *Neurotoxicology* 2013; **39**: 11–17.
- 21 Needleman HL, Riess JA, Tobin MJ, Biesecker GE, Greenhouse JB. Bone lead levels and delinquent behavior. *JAMA* 1996; **275**: 363–369.
- 22 Peters JL, Kubzansky LD, Ikeda A, Spiro A 3rd, Wright RO, Weisskopf MG *et al*. Childhood and adult socioeconomic position, cumulative lead levels, and pessimism in later life: the VA Normative Aging Study. *Am J Epidemiol* 2011; **174**: 1345–1353.
- 23 Wright JP, Dietrich KN, Ris MD, Hornung RW, Wessel SD, Lanphear BP *et al*. Association of prenatal and childhood blood lead concentrations with criminal arrests in early adulthood. *PLoS Med* 2008; **5**: e101.
- 24 Opler MG, Brown AS, Graziano J, Desai M, Zheng W, Schaefer C *et al*. Prenatal lead exposure, delta-aminolevulinic acid, and schizophrenia. *Environ Health Perspect* 2004; **112**: 548–552.
- 25 Opler MG, Buka SL, Groeger J, McKeague I, Wei C, Factor-Litvak P *et al*. Prenatal exposure to lead, delta-aminolevulinic acid, and schizophrenia: further evidence. *Environ Health Perspect* 2008; **116**: 1586–1590.
- 26 Cecil KM, Brubaker CJ, Adler CM, Dietrich KN, Altaye M, Egelhoff JC *et al*. Decreased brain volume in adults with childhood lead exposure. *PLoS Med* 2008; **5**: e112.
- 27 Schwartz BS, Stewart WF, Bolla KI, Simon PD, Bandeen-Roche K, Gordon PB *et al*. Past adult lead exposure is associated with longitudinal decline in cognitive function. *Neurology* 2000; **55**: 1144–1150.
- 28 Stewart WF, Schwartz BS, Davatzikos C, Shen D, Liu D, Wu X *et al*. Past adult lead exposure is linked to neurodegeneration measured by brain MRI. *Neurology* 2006; **66**: 1476–1484.
- 29 Stewart WF, Schwartz BS. Effects of lead on the adult brain: a 15-year exploration. *Am J Ind Med* 2007; **50**: 729–739.
- 30 Brubaker CJ, Dietrich KN, Lanphear BP, Cecil KM. The influence of age of lead exposure on adult gray matter volume. *Neurotoxicology* 2010; **31**: 259–266.
- 31 Brubaker CJ, Schmithorst VJ, Haynes EN, Dietrich KN, Egelhoff JC, Lindquist DM *et al*. Altered myelination and axonal integrity in adults with childhood lead exposure: a diffusion tensor imaging study. *Neurotoxicology* 2009; **30**: 867–875.
- 32 Guilarte TR, Opler M, Pletnikov M. Is lead exposure in early life an environmental risk factor for Schizophrenia? Neurobiological connections and testable hypotheses. *Neurotoxicology* 2012; **33**: 560–574.
- 33 Abazyan B, Dziedzic J, Hua K, Abazyan S, Yang C, Mori S *et al*. Chronic exposure of mutant DISC1 mice to lead produces sex-dependent abnormalities consistent with schizophrenia and related mental disorders: a gene-environment interaction study. *Schizophr Bull* 2014; **40**: 575–584.
- 34 Olney JW, Farber NB. Glutamate receptor dysfunction and schizophrenia. *Arch Gen Psychiatry* 1995; **52**: 998–1007.
- 35 Coyle JT, Tsai G. NMDA receptor function, neuroplasticity, and the pathophysiology of schizophrenia. *Int Rev Neurobiol* 2004; **59**: 491–515.
- 36 Snyder MA, Gao WJ. NMDA hypofunction as a convergence point for progression and symptoms of schizophrenia. *Front Cell Neurosci* 2013; **7**: 31.
- 37 Alkondon M, Costa AC, Radhakrishnan V, Aronstam RS, Albuquerque EX. Selective blockade of NMDA-activated channel currents may be implicated in learning deficits caused by lead. *FEBS Lett* 1990; **261**: 124–130.
- 38 Guilarte TR, Miceli RC. Age-dependent effects of lead on [3H]MK-801 binding to the NMDA receptor-gated ionophore: *in vitro* and *in vivo* studies. *Neurosci Lett* 1992; **148**: 27–30.
- 39 Gavazzo P, Zanardi I, Baranowska-Bosiacka I, Marchetti C. Molecular determinants of Pb2+ interaction with NMDA receptor channels. *Neurochem Int* 2008; **52**: 329–337.
- 40 Toscano CD, Hashemzadeh-Gargari H, McGlothlan JL, Guilarte TR. Developmental Pb2+ exposure alters NMDAR subtypes and reduces CREB phosphorylation in the rat brain. *Brain Res Dev Brain Res* 2002; **139**: 217–226.
- 41 Toscano CD, Guilarte TR. Lead neurotoxicity: from exposure to molecular effects. *Brain Res Brain Res Rev* 2005; **49**: 529–554.
- 42 Sheng M, Cummings J, Roldan LA, Jan YN, Jan LY. Changing subunit composition of heteromeric NMDA receptors during development of rat cortex. *Nature* 1994; **368**: 144–147.
- 43 Quinlan EM, Philpot BD, Hagan RL, Bear MF. Rapid, experience-dependent expression of synaptic NMDA receptors in visual cortex *in vivo*. *Nat Neurosci* 1999; **2**: 352–357.
- 44 Bellone C, Nicoll RA. Rapid bidirectional switching of synaptic NMDA receptors. *Neuron* 2007; **55**: 779–785.
- 45 Matta JA, Ashby MC, Sanz-Clemente A, Roche KW, Isaac JT. mGluR5 and NMDA receptors drive the experience- and activity-dependent NMDA receptor NR2B to NR2A subunit switch. *Neuron* 2011; **70**: 339–351.
- 46 Nihei MK, Desmond NL, McGlothlan JL, Kuhlmann AC, Guilarte TR. N-methyl-D-aspartate receptor subunit changes are associated with lead-induced deficits of long-term potentiation and spatial learning. *Neuroscience* 2000; **99**: 233–242.
- 47 McGlothlan JL, Karcz-Kubicha M, Guilarte TR. Developmental lead exposure impairs extinction of conditioned fear in young adult rats. *Neurotoxicology* 2008; **29**: 1127–1130.
- 48 Hashimoto T, Volk DW, Eggan SM, Mirnics K, Pierri JN, Sun Z *et al*. Gene expression deficits in a subclass of GABA neurons in the prefrontal cortex of subjects with schizophrenia. *J Neurosci* 2003; **23**: 6315–6326.
- 49 Hashimoto T, Bazmi HH, Mirnics K, Wu Q, Sampson AR, Lewis DA. Conserved regional patterns of GABA-related transcript expression in the neocortex of subjects with schizophrenia. *Am J Psychiatry* 2008; **165**: 479–489.
- 50 Lewis DA, Gonzalez-Burgos G. Pathophysiologically based treatment interventions in schizophrenia. *Nat Med* 2006; **12**: 1016–1022.
- 51 Mellios N, Huang HS, Baker SP, Galdzicka M, Ginns E, Akbarian S. Molecular determinants of dysregulated GABAergic gene expression in the prefrontal cortex of subjects with schizophrenia. *Biol Psychiatry* 2009; **65**: 1006–1014.
- 52 Fung SJ, Webster MJ, Sivagnanasundaram S, Duncan C, Elashoff M, Weickert CS. Expression of interneuron markers in the dorsolateral prefrontal cortex of the developing human and in schizophrenia. *Am J Psychiatry* 2010; **167**: 1479–1488.
- 53 Volk DW, Matsubara T, Li S, Sengupta EJ, Georgiev D, Minabe Y *et al*. Deficits in transcriptional regulators of cortical parvalbumin neurons in schizophrenia. *Am J Psychiatry* 2012; **169**: 1082–1091.
- 54 Uhlhaas PJ, Singer W. Abnormal neural oscillations and synchrony in schizophrenia. *Nat Rev Neurosci* 2010; **11**: 100–113.
- 55 Volman V, Behrens MM, Sejnowski TJ. Downregulation of parvalbumin at cortical GABA synapses reduces network gamma oscillatory activity. *J Neurosci* 2011; **31**: 18137–18148.
- 56 Gandal MJ, Sisti J, Klook K, Ortinski PI, Leitman V, Liang Y *et al*. GABAB-mediated rescue of altered excitatory-inhibitory balance, gamma synchrony and behavioral deficits following constitutive NMDAR-hypofunction. *Transl Psychiatry* 2012; **2**: e142.

- 57 Kocsis B. Differential role of NR2A and NR2B subunits in *N*-methyl-D-aspartate receptor antagonist-induced aberrant cortical gamma oscillations. *Biol Psychiatry* 2012; **71**: 987–995.
- 58 Belforte JE, Zsiros V, Sklar ER, Jiang Z, Yu G, Li Y *et al*. Postnatal NMDA receptor ablation in corticolimbic interneurons confers schizophrenia-like phenotypes. *Nat Neurosci* 2010; **13**: 76–83.
- 59 Cochran SM, Fujimura M, Morris BJ, Pratt JA. Acute and delayed effects of phencyclidine upon mRNA levels of markers of glutamatergic and GABAergic neurotransmitter function in the rat brain. *Synapse* 2002; **46**: 206–214.
- 60 Keilhoff G, Becker A, Grecksch G, Wolf G, Bernstein HG. Repeated application of ketamine to rats induces changes in the hippocampal expression of parvalbumin, neuronal nitric oxide synthase and cFOS similar to those found in human schizophrenia. *Neuroscience* 2004; **126**: 591–598.
- 61 Abekawa T, Ito K, Nakagawa S, Koyama T. Prenatal exposure to an NMDA receptor antagonist, MK-801 reduces density of parvalbumin-immunoreactive GABAergic neurons in the medial prefrontal cortex and enhances phencyclidine-induced hyperlocomotion but not behavioral sensitization to methamphetamine in postpubertal rats. *Psychopharmacology (Berl)* 2007; **192**: 303–316.
- 62 Kittelberger K, Hur EE, Sazegar S, Keshavan V, Kocsis B. Comparison of the effects of acute and chronic administration of ketamine on hippocampal oscillations: relevance for the NMDA receptor hypofunction model of schizophrenia. *Brain Struct Funct* 2012; **217**: 395–409.
- 63 Kaalund SS, Riise J, Broberg BV, Fabricius K, Karlens AS, Secher T *et al*. Differential expression of parvalbumin in neonatal phencyclidine-treated rats and socially isolated rats. *J Neurochem* 2013; **124**: 548–557.
- 64 Carlsson A. The neurochemical circuitry of schizophrenia. *Pharmacopsychiatry* 2006; **39 Suppl 1**: S10–S14.
- 65 Laruelle M, Abi-Dargham A, van Dyck CH, Gil R, D'Souza CD, Erdos J *et al*. Single photon emission computerized tomography imaging of amphetamine-induced dopamine release in drug-free schizophrenic subjects. *Proc Natl Acad Sci USA* 1996; **93**: 9235–9240.
- 66 Breier A, Su TP, Saunders R, Carson RE, Kolachana BS, de Bartolomeis A *et al*. Schizophrenia is associated with elevated amphetamine-induced synaptic dopamine concentrations: evidence from a novel positron emission tomography method. *Proc Natl Acad Sci USA* 1997; **94**: 2569–2574.
- 67 Abi-Dargham A, Gil R, Krystal J, Baldwin RM, Seibyl JP, Bowers M *et al*. Increased striatal dopamine transmission in schizophrenia: confirmation in a second cohort. *Am J Psychiatry* 1998; **155**: 761–767.
- 68 Abi-Dargham A, van de Giessen E, Slifstein M, Kegeles LS, Laruelle M. Baseline and amphetamine-stimulated dopamine activity are related in drug-naive schizophrenic subjects. *Biol Psychiatry* 2009; **65**: 1091–1093.
- 69 Lodge DJ, Grace AA. Hippocampal dysregulation of dopamine system function and the pathophysiology of schizophrenia. *Trends Pharmacol Sci* 2011; **32**: 507–513.
- 70 Del Arco A, Segovia G, Mora F. Blockade of NMDA receptors in the prefrontal cortex increases dopamine and acetylcholine release in the nucleus accumbens and motor activity. *Psychopharmacology (Berl)* 2008; **201**: 325–338.
- 71 Dorph-Petersen KA, Lewis DA. Stereological approaches to identifying neuropathology in psychosis. *Biol Psychiatry* 2011; **69**: 113–126.
- 72 Sheleg M, Yochum CL, Wagner GC, Zhou R, Richardson JR. Ephrin-A5 deficiency alters sensorimotor and monoaminergic development. *Behav Brain Res* 2013; **236**: 139–147.
- 73 Grace AA. Dopamine system dysregulation by the ventral subiculum as the common pathophysiological basis for schizophrenia psychosis, psychostimulant abuse, and stress. *Neurotox Res* 2010; **18**: 367–376.
- 74 Gether U, Andersen PH, Larsson OM, Schousboe A. Neurotransmitter transporters: molecular function of important drug targets. *Trends Pharmacol Sci* 2006; **27**: 375–383.
- 75 Akbarian S, Kim JJ, Potkin SG, Hagman JO, Tafazzoli A, Bunney WE Jr. *et al*. Gene expression for glutamic acid decarboxylase is reduced without loss of neurons in prefrontal cortex of schizophrenics. *Arch Gen Psychiatry* 1995; **52**: 258–266.
- 76 Bitanihirwe BK, Lim MP, Kelley JF, Kaneko T, Woo TU. Glutamatergic deficits and parvalbumin-containing inhibitory neurons in the prefrontal cortex in schizophrenia. *BMC Psychiatry* 2009; **9**: 71.
- 77 Beasley CL, Zhang ZJ, Patten I, Reynolds GP. Selective deficits in prefrontal cortical GABAergic neurons in schizophrenia defined by the presence of calcium-binding proteins. *Biol Psychiatry* 2002; **52**: 708–715.
- 78 Volk DW, Austin MC, Pierri JN, Sampson AR, Lewis DA. Decreased glutamic acid decarboxylase67 messenger RNA expression in a subset of prefrontal cortical gamma-aminobutyric acid neurons in subjects with schizophrenia. *Arch Gen Psychiatry* 2000; **57**: 237–245.
- 79 Zhang ZJ, Reynolds GP. A selective decrease in the relative density of parvalbumin-immunoreactive neurons in the hippocampus in schizophrenia. *Schizophr Res* 2002; **55**: 1–10.
- 80 Beasley CL, Reynolds GP. Parvalbumin-immunoreactive neurons are reduced in the prefrontal cortex of schizophrenics. *Schizophr Res* 1997; **24**: 349–355.
- 81 Braun I, Genius J, Grunze H, Bender A, Moller HJ, Rujescu D. Alterations of hippocampal and prefrontal GABAergic interneurons in an animal model of psychosis induced by NMDA receptor antagonism. *Schizophr Res* 2007; **97**: 254–263.
- 82 Sadiqot AF, Burhan AM, Belanger MC, Sasseville R. NMDA receptor antagonists influence early development of GABAergic interneurons in the mammalian striatum. *Brain Res Dev Brain Res* 1998; **105**: 35–42.
- 83 Nihei MK, Guilarte TR. NMDAR-2A subunit protein expression is reduced in the hippocampus of rats exposed to Pb2+ during development. *Brain Res Mol Brain Res* 1999; **66**: 42–49.
- 84 Kinney JW, Davis CN, Tabarean I, Conti B, Bartfai T, Behrens MM. A specific role for NR2A-containing NMDA receptors in the maintenance of parvalbumin and GAD67 immunoreactivity in cultured interneurons. *J Neurosci* 2006; **26**: 1604–1615.
- 85 Xi D, Keeler B, Zhang W, Houle JD, Gao WJ. NMDA receptor subunit expression in GABAergic interneurons in the prefrontal cortex: application of laser microdissection technique. *J Neurosci Methods* 2009; **176**: 172–181.
- 86 Buhl EH, Szilagyi T, Halasy K, Somogyi P. Physiological properties of anatomically identified basket and bistratified cells in the CA1 area of the rat hippocampus *in vitro*. *Hippocampus* 1996; **6**: 294–305.
- 87 Grunze HC, Rainnie DG, Hasselmo ME, Barkai E, Hearn EF, McCarley RW *et al*. NMDA-dependent modulation of CA1 local circuit inhibition. *J Neurosci* 1996; **16**: 2034–2043.
- 88 Xi D, Zhang W, Wang HX, Stradtman GG, Gao WJ. Dizocilpine (MK-801) induces distinct changes of *N*-methyl-D-aspartic acid receptor subunits in parvalbumin-containing interneurons in young adult rat prefrontal cortex. *Int J Neuropsychopharmacol* 2009; **12**: 1395–1408.
- 89 Zhang Z, Sun QQ. Development of NMDA NR2 subunits and their roles in critical period maturation of neocortical GABAergic interneurons. *Dev Neurobiol* 2011; **71**: 221–245.
- 90 Seeman P. Schizophrenia and dopamine receptors. *Eur Neuropsychopharmacol* 2013; **23**: 999–1009.
- 91 Jaaro-Peled H, Niwa M, Foss CA, Murai R, de Los Reyes S, Kamiya A *et al*. Subcortical dopaminergic deficits in a DISC1 mutant model: a study in direct reference to human molecular brain imaging. *Hum Mol Genet* 2013; **22**: 1574–1580.
- 92 Zuch CL, O'Mara DJ, Cory-Slechta DA. Low-level lead exposure selectively enhances dopamine overflow in nucleus accumbens: an *in vivo* electrochemistry time course assessment. *Toxicol Appl Pharmacol* 1998; **150**: 174–185.
- 93 Brunelin J, Fecteau S, Suaud-Chagny MF. Abnormal striatal dopamine transmission in schizophrenia. *Curr Med Chem* 2013; **20**: 397–404.
- 94 Verina T, Rohde CA, Guilarte TR. Environmental lead exposure during early life alters granule cell neurogenesis and morphology in the hippocampus of young adult rats. *Neuroscience* 2007; **145**: 1037–1047.
- 95 Commissaris RL, Tavakoli-Nezhad M, Barron AJ, Pitts DK. Effects of chronic low-level oral lead exposure on prepulse inhibition of acoustic startle in the rat. *Neurotoxicol Teratol* 2000; **22**: 55–60.
- 96 Guilarte TR, Toscano CD, McGlothlan JL, Weaver SA. Environmental enrichment reverses cognitive and molecular deficits induced by developmental lead exposure. *Ann Neurol* 2003; **53**: 50–56.
- 97 Clune AL FH, Riederer AM. Mapping global environmental lead poisoning in children. *J Health Pollut* 2011; **1**: 16–25.



This work is licensed under a Creative Commons Attribution-NonCommercial-ShareAlike 4.0 International License. The images or other third party material in this article are included in the article's Creative Commons license, unless indicated otherwise in the credit line; if the material is not included under the Creative Commons license, users will need to obtain permission from the license holder to reproduce the material. To view a copy of this license, visit <http://creativecommons.org/licenses/by-nc-sa/4.0/>

Supplementary Information accompanies the paper on the Translational Psychiatry website (<http://www.nature.com/tp>)